ARTICLE   OPEN

Check for updates

Performance and mechanisms of greywater treatment in a bio-enhanced granular-activated carbon dynamic biofilm reactor

Ziqi Wang[1,2], Ying Yang[1,2], Wanchen Xiang[1,2], Beibei Wu[1], Xiaocai Cui[1] and Yun Zhou [1 ✉]

The potential of source-diverted graywater reuse mainly relies on the efficiency and cost of graywater treatment technology. Oxygen (O_2) supply and utilization rate directly determine the energy consumption and pollutants removal rate in the biological graywater treatment. This study developed a gravity flow self-supplying O_2 and easy-to-maintain bio-enhanced granular-activated carbon dynamic biofilm reactor (BhGAC-DBfR) for on-site graywater treatment. Results showed that increasing of saturated/unsaturated ratio led to the continuous growth of biomass on GAC surface. Division of saturated and unsaturated zones favors the formation of aerobic-anoxic-anaerobic biofilm in the reactor. A saturated/unsaturated ratio of 1:1.1 achieved the maximum removal rate of chemical oxygen demand (COD), linear alkylbenzene sulfonates (LAS), ammonia nitrogen, and total nitrogen at 98.3%, 99.4%, 99.8%, and 83.5%, respectively. Key is that adsorption and biodegradation play important and distinct roles in the quick uptake and continuous removal of both organics and N in the system. The related genus and enzymes functional for LAS mineralization, deamination of organic N, ammonium oxidation, and nitrate respiration enabled the efficient and simultaneous removal of organics and N in the BhGAC-DBfR. This study offers a promising engineering alternative technology with great potential to achieve efficient and low-energy-input graywater treatment.

npj Clean Water (2022)5:56 ; https://doi.org/10.1038/s41545-022-00198-7

INTRODUCTION

Increasing demand for fresh water has led to efforts in conserving precious water resources and reusing wastewater[1]. As the main source of domestic sewage (50–80%), graywater is defined as wastewater generated from households, excluding that from toilets[2]. As mainly produced from daily washing and cleaning, graywater always contains nitrogen, pathogens, micropollutants, and a high concentration of linear alkylbenzene sulfonates (LAS)[3]. The on-site treatment and reuse of source-diverted graywater have attracted wide attention nowadays, which can reduce the transportation and treatment cost of wastewater[4,5]. Thus, GW treatment and reuse are significant for both environmental protection and the sustainable development of water resources[6].

Various methods, including physical, chemical, biological, and combined techniques, have been used to treat graywater[1,7]. However, low efficiency and quality of treated effluent and high energy input limit the extensive application of on-site decentralized graywater[8]. Traditional aerobic biological treatment technologies can achieve efficient removal of organics and nitrogen[3], but several shortcomings still remain. High LAS concentration in graywater causes serious foaming during blast aeration, which may lead to biomass loss and the declined reactor performance[9]; moreover, direct gas bubbling always has low oxygen (O_2)-transfer and utilization rates[10], which increases the graywater treatment cost. Recently, the oxygen-based membrane biofilm reactor (O_2-MBfR) was applied for graywater treatment, and O_2 is the electron acceptor and supplied from the air; This system completely avoids foaming formation and achieves an extremely high O_2 transfer rate, as well as enables the efficient removal of both organics and nitrogen[11,12]. However, pressurized air transfer determines the high graywater treatment cost in the O_2-MBfR; long-term operation of the system requires regular leakage detection and replacement of membrane module, as well

as the ventilation and drainage for membrane anti-blocking, all of which increase the system maintenance cost. Because of the high porosity, large specific surface area, and excellent adsorption property, granular-activated carbon (GAC) is widely used as the filter media for biological filters in wastewater treatment[13]. In the GAC-based biofilters, GAC media can enable the attachment and growth of biofilm[8]; as the "pollutants transfer station", GAC can also uptake and store various pollutants that supply microbial metabolism[14], all of which maintain high activity and biochemical reaction rate in the biofilm. GAC biofilters can achieve the efficient removal of pollutants by multiple processes, including GAC filtration, adsorption, and catalysis[14], as well as the biosorption and biodegradation in biofilm[15]. Therefore, the combination of GAC combined with biofilm may significantly improve the pollutants removal efficiency and reduce the energy input of graywater treatment.

Despite the wide application of GAC biofilter in municipal wastewater treatment, little is known about the formation, physicochemical properties, and microbial ecology of GAC-biofilm, as well as the pollutants removal-related function genes and enzymes during graywater treatment. In this study, we propose to develop a bio-enhanced granular-activated carbon dynamic biofilm reactor (BhGAC-DBfR) for source-diverted graywater treatment. Division of saturated and unsaturated zones inside the reactor is conducive to the formation of aerobic-anoxic-anaerobic biofilm, which enables the efficient and simultaneous removal of organics and nitrogen. The dynamics of biofilm morphology, components concentrations, and functional groups were investigated. The variations of COD, LAS, ammonium, and TN removal in response to changes in saturated/unsaturated zone ratio (based on volume) were studied. The adsorption and biodegradation of LAS in this system were distinguished and quantified. The fate of related genes and enzymes functional for

[1]State Environmental Protection Key Laboratory of Soil Health and Green Remediation, College of Resources and Environment, Huazhong Agricultural University, 430070 Wuhan, China. [2]These authors contributed equally: Ziqi Wang, Ying Yang, Wanchen Xiang. ✉email: yzhou112@mail.hzau.edu.cn

npj

organics and nitrogen removal were tracked. It is expected that the proposed BhGAC-DBfR could offer a feasible engineering application technology for achieving efficient and low-energy-input graywater treatment.

RESULTS

Biofilm characteristics

GAC is an excellent carrier for biofilm growth, which can quickly uptake organics and nutrients from the liquid phase for the metabolism of microorganisms in the biofilm[15,16]. Figure 1 shows the dynamics of GAC morphology with and without biofilm, concentrations of biofilm components, and functional groups at different positions of the reactor. The elements in the fresh GAC mainly include carbon (C, 88.4%), nitrogen (N, 4.87%), oxygen (O, 5.68%), and a smaller amount of phosphorus (P, 0.04%), and the GAC surface is relatively smooth. After the formation of biofilm, GAC surface was attached by a large amount of biomass, which becomes rougher. The proportions of dominant elements, including N, O, and P, significantly increased due to the accumulation of protein, carbohydrate,s and DNA in the biofilm (Fig. 1e). Notably, the sulfur element was also detected, which should be contributed to the adsorption of LAS (sulfonic acid group) by GAC and biofilm[17,18].

As shown in Fig. 1f, the concentrations of protein, carbohydrate, and DNA gradually increased with the increasing of saturated/unsaturated ratio. At each phase, the total concentration of components at the top of the reactor was much higher than that at the stratification and bottom of the system, leading to the relatively high elements proportions of N, O, and P in the biofilm (Fig. 1b). The concentrations of protein and carbohydrate were much higher than DNA in the biofilm at each phase. Previous studies indicated that protein- and carbohydrate-enriched extracellular polymeric substances (EPS) improved the accumulation of LAS in biofilm[18]; moreover, protein-enriched EPS can achieve short-time protection of biofilm from LAS toxicity to microbial physiological functions[19], all of which maintained stable biofilm structure and efficient LAS removal in the system.

Figure 1g shows the 2D-FTIR correlation synchronous and asynchronous maps of the biofilms at the noted reactor positions. In both synchronous and asynchronous maps, the functional groups at the top and the stratification of the reactor were quite similar. The top and stratification synchronous map of 600–2000 cm^{-1} region (Fig. 1g) both contains four positive autopeaks at 1120, 1410, 1583, and 1770 cm^{-1} and two crosspeak at (1770, 1120) cm^{-1} and (1575,1120) cm^{-1}. The highest intensity change at 1120 cm^{-1} showed that C–O was more sensitive than C=O and N–H to biofilm from different positions of BhGAC-DBfR. Meanwhile, the top asynchronous map of 600–2000 cm^{-1} region displays two positive crosspeaks at (1770, 1120) cm^{-1} and (1660, 1120) cm^{-1}, and two negative crosspeaks at (1600, 1120) cm^{-1} and (1210, 1645) cm^{-1}. Based on the Noda's rule[20], the dynamics of N–H at the top was predominant than C=O, RCONHR', and amide II. The bottom synchronous map of 600–2000 cm^{-1} region contains two positive autopeaks at 600 and 1410 cm^{-1} and three crosspeak at (1410, 600) cm^{-1}, (1591, 600) cm^{-1}, and (1591, 1410) cm^{-1}. The higher intensity change at 600 cm^{-1} showed that aliphatic ketone was more sensitive than amide II and N–H to the bottom biofilm. Moreover, the bottom asynchronous map of 600–2000 cm^{-1} region displays four positive crosspeaks at (1696, 600) cm^{-1}, (1533, 600) cm^{-1}, (1696, 1410) cm^{-1}, and (1533, 1410) cm^{-1}, which indicates that the dynamics of aliphatic ketone at the bottom was predominant than N–H, amide II, and RCONHR'. Multifarious functional groups in the biofilm also allowed adsorption and accumulation of both organics and nitrogen for bio-removal in the bio-enhanced GAC, which enabled the stable performance of BhGAC-DBfR during graywater treatment.

Reactor performance

Figure 2 shows the removal of COD, LAS, NH$_4^+$−N, and TN, as well as the dynamics of pH value for different saturated/unsaturated ratios in the BhGAC-DBfR treating graywater. In Phase II, with the saturated/unsaturated ratio of 1:1.1, the system achieved the best performance overall: the lowest effluent concentrations and greatest removals of COD (98.0%), LAS (98.4%), NH$_4^+$−N (99.3%), and TN (83.5%). The saturated zone enabled the further removal of all the mentioned contaminants as the reactor effluent concentration was lower than that in the stratification effluent for each of the items. A much higher saturated/unsaturated ratio (1:0.5) in Phase III reduced the influent oxygenation height and time, leading to the decreased DO concentrations in the stratification (0.84 ± 0.02 mg/L) and effluent (0.08 ± 0.01 mg/L) of the reactor. Insufficient DO lead to incomplete organics biodegradation and ammonia oxidation in the system[21]. Moreover, the pH values of the unsaturated and reactor effluent were higher than the influent pH (7.05 ± 0.05) in Phase I, which further indicated that the multiple function layers of biofilm enabled the denitrification in both saturated and unsaturated zones of the BhGAC-DBfR. Because of the same HRT in each Phase, a high saturated/unsaturated ratio led to fast inflow velocity and high organics and ammonium loading rates (Table 1); complete ammonia oxidation in the unsaturated zone led to the decrease of pH value in the unsaturated effluent (Fig. 2e).

Differentiation and quantification of LAS adsorption and biodegradation

Figure 3 shows the removal kinetics of LAS in fresh GAC, inactivated biofilm-GAC, and bio-enhanced GAC, as well as the modeling results of biodegraded and biofilm-attached LAS in the bio-enhanced GAC; Table 2 presents the related parameters of the adsorption and biodegradation kinetics during batch-mode LAS removal. The porous structure (Fig. 1a–d) and multifarious function groups (Fig. 1g) in both GAC and biofilm enabled the adsorption and accumulation of LAS in the GAC-biofilm system[22]. For the adsorption of LAS in both fresh GAC and inactivated GAC, the pseudo-first-order model fitted the experimental data well due to the relatively low SSE values and the fairly satisfactory results between $q_{e, mod}$ and $q_{r, exp}$. Results indicated that LAS adsorption in the GAC-biofilm follows the interior surface adsorption model[23]. In the bio-enhanced GAC system, a two-step removal model including biofilm adsorption and biodegradation was used for the simulation of LAS removal[17]. The model results for the residual LAS in the solution match well with the experimental data due to low P-values (<0.01) for all the simulations, which achieved the LAS biodegradation rate constant of 0.0580 h^{-1} in the bio-enhanced GAC. Moreover, the adsorption rate constant and the equilibrium adsorption capacity of LAS in fresh GAC are higher than that in the inactivated GAC, indicating the excellent adsorption performance of fresh GAC and biofilm attachment will partly reduce the adsorption capacity of GAC. LAS in the bio-enhanced GAC showed a rapid accumulation initially and then gradually decreased due to the biodegradation[14,17]. Key is that adsorption and biodegradation play important and distinct roles in the quick uptake and continuous removal of both LAS and nitrogen in the system.

Microbial community diversity and composition

Figure 4a shows a PCoA based on Bray-Curtis distance matrices representing the distributions of the bacterial communities at different reactor positions and operation Phases. The biofilms collected from the top and stratification of the BhGAC-DBfR formed similar clusters; however, biofilms at the bottom of the reactor had a distinct cluster compared with other communities on the PCoA2 axis (25.7%). Results indicated that the community structure of the biofilm at the reactor bottom was markedly
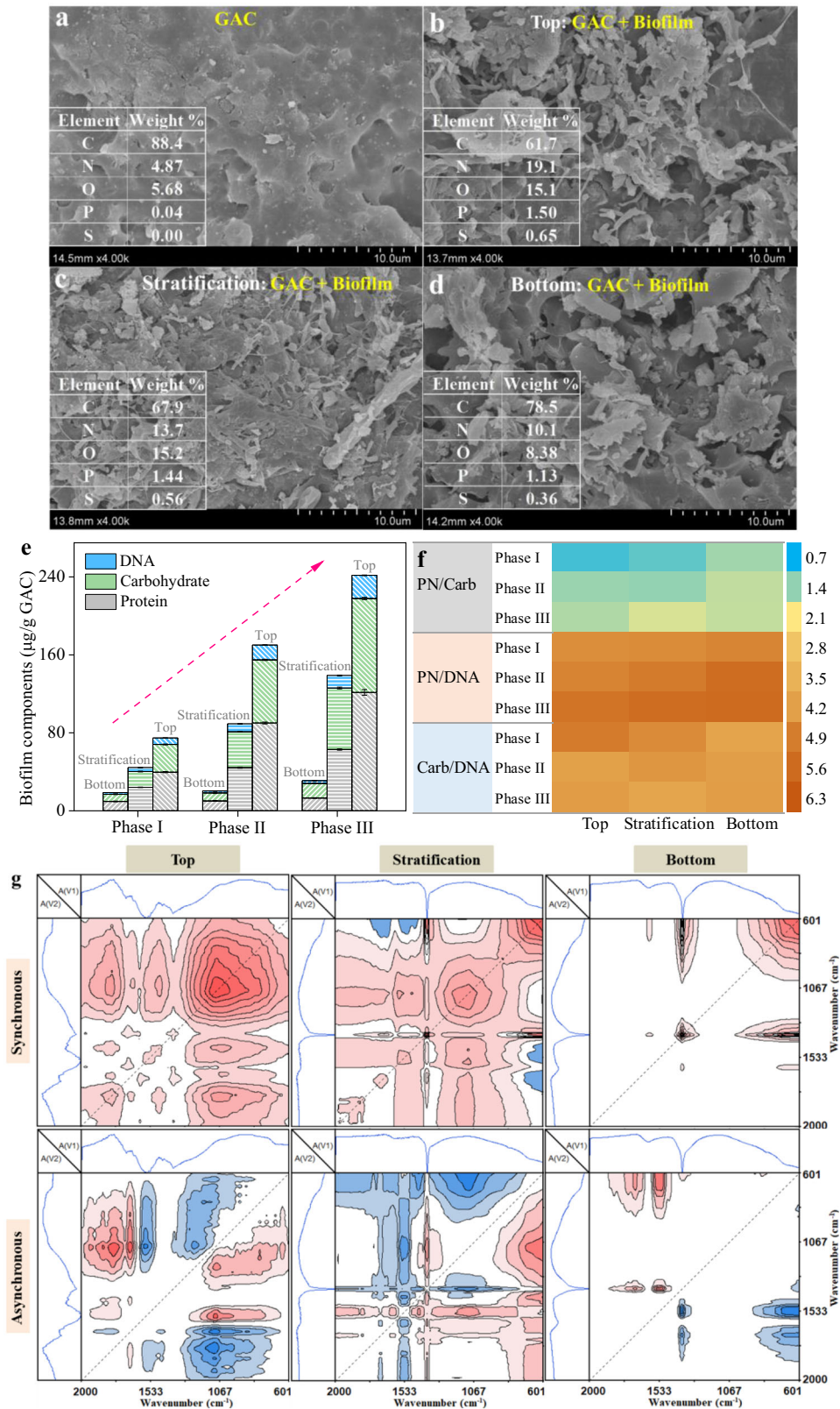
Fig. 1 Biofilm characteristics. Dynamics of biofilm characteristics represented by **a**–**d** the surface morphology and the element sidtribution of the granular-activated carbon and biofilm using scanning electron microscope (SEM) combined with energy dispersive X-ray (EDX) spectrometry, **e** biofilm components containing protein, carbohydrate and DNA and **f** component ratios, and **g** the two dimension (2D)-FTIR correlation synchronous and asynchronous maps generated from 600–2000 cm^{-1} region of the biofilms at the noted reactor position and operation Phase. Red represents positive correlations and blue represents negative correlations; higher color intensity indicates a stronger positive or negative correlation. Phases I, II, and III represent the saturated/unsaturated ratio of 1:2.3, 1:1.1, and 1:0.5, respectively.
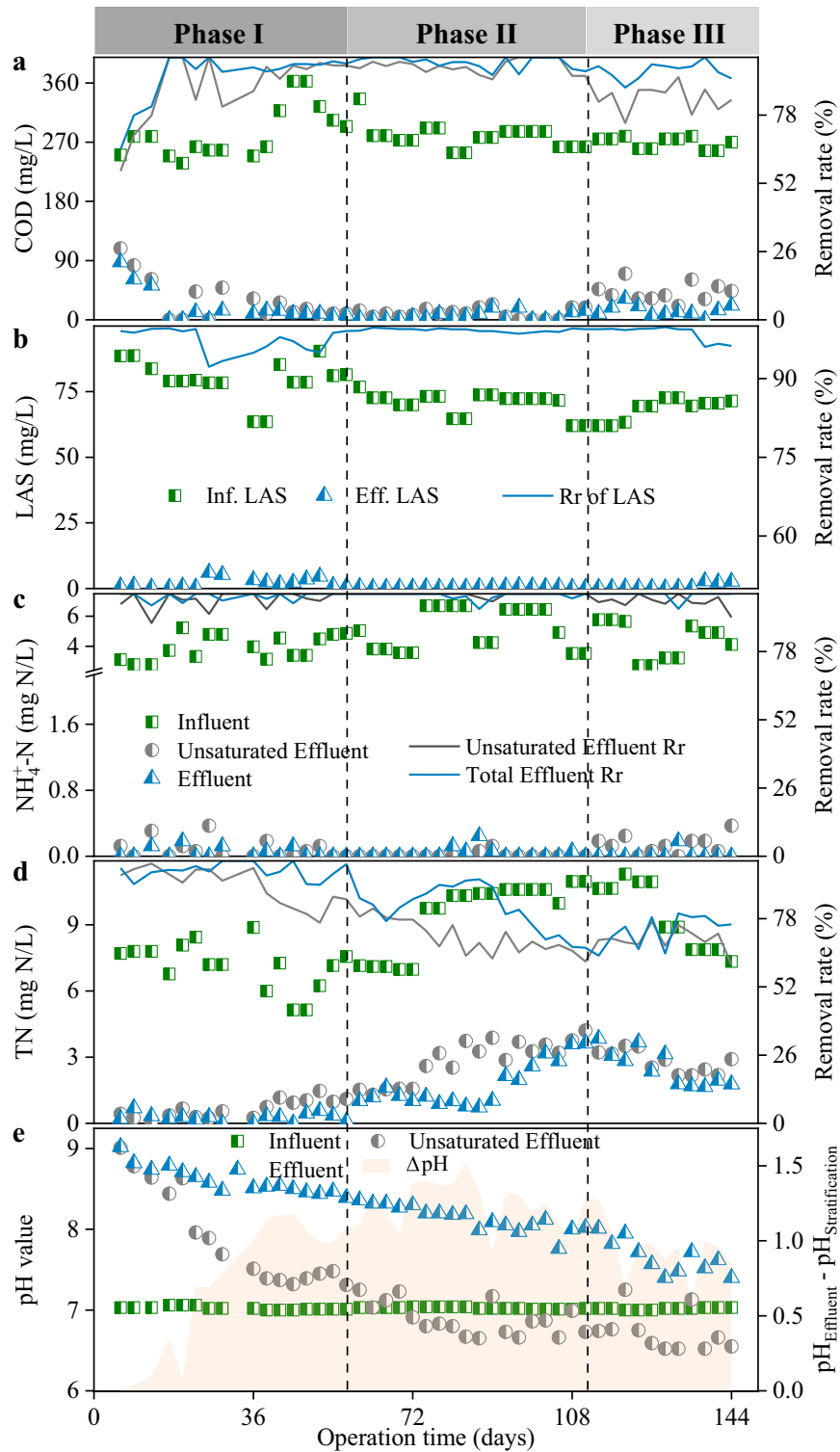
Fig. 2 Reactor performances. Dynamics of the removal of **a** COD, **b** LAS, **c** NH$_4^+$−N, **d** TN, and **e** pH at different Phases in the bio-enhanced granular-activated carbon dynamic biofilm reactor (BhGAC-DBfR) during graywater treatment. Phases I, II, and III represent the saturated/unsaturated ratio of 1:2.3, 1:1.1, and 1:0.5, respectively.

different from the upside, which probably is relevant to the relatively low DO concentration at the bottom of the reactor (Table 1), and lower DO lead to a more distant of the community cluster (Fig. 4a).

Figure 4b presents the mean proportion and the differences among the bacteria in the top and stratification, as well as between

the stratification and bottom in the reactor. Results further confirmed the similar biofilm community compositions at the top and stratification of the reactor; the dominant bacteria in both positions were α-Proteobacteria and γ-Proteobacteria, which were involved in the organics oxidation and nitrogen transformation processes[24,25]. Almost the similar relative abundance of Nitrospira in

Table 1. Operation conditions of the BhGAC-DBfR[a] and the dissolved oxygen dynamics for all Phases.

Phase	Saturated/unsaturated	HLR[b] (L/(m²·d))	OLR[c] (gCOD/(m²·d))	DO$_{Inf.}$[d] (mg/L)	DO$_{Strat.}$[e] (mg/L)	DO$_{Eff.}$[f] (mg/L)
I	1:2.3	358	101.7 ± 12.5	0.00 ± 0.00	1.71 ± 0.03	0.26 ± 0.02
II	1:1.1	563	157.6 ± 11.8	0.01 ± 0.01	1.24 ± 0.05	0.15 ± 0.02
III	1:0.4	844	230.4 ± 10.9	0.00 ± 0.00	0.84 ± 0.02	0.08 ± 0.01

[a]BhGAC-DBfR is bio-enhanced granular-activated carbon dynamic biofilm reactor.
[b]HLR is hydraulic loading rate.
[c]OLR is organic loading rate.
[d]DO is dissolved oxygen.
DO$_{Inf.}$[d], DO$_{Strat.}$[e], and DO$_{Eff.}$[f] are dissolved oxygen concentrations in the influent, stratification, and effluent, respectively.
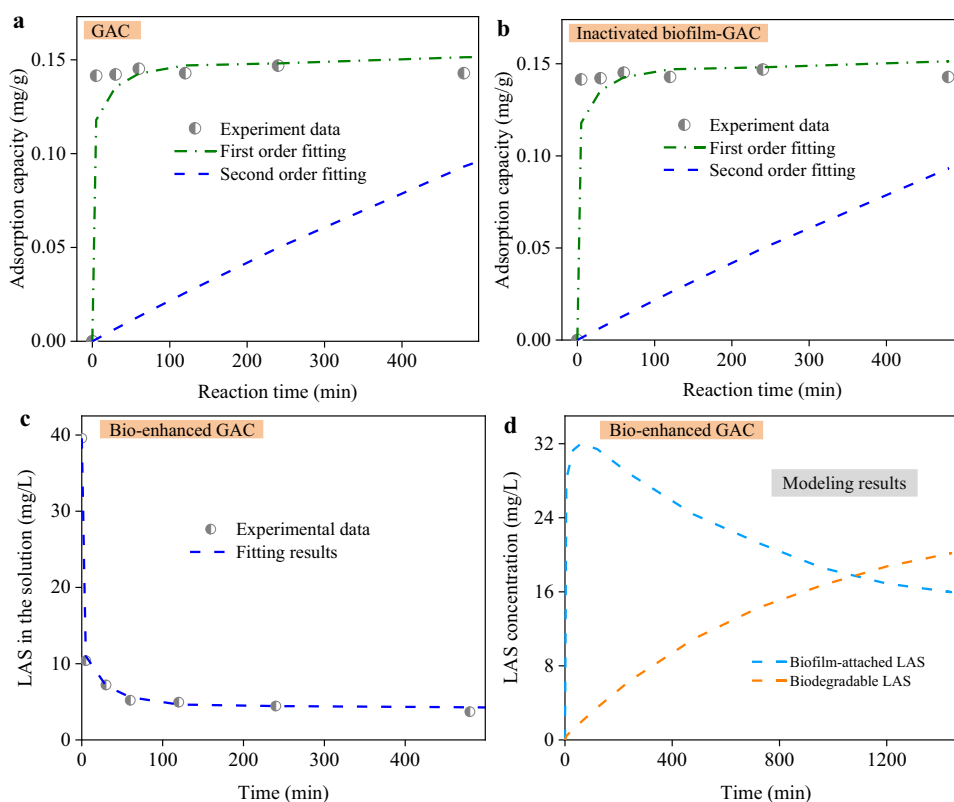

Fig. 3 LAS removal kinetics. Batch experiments for the removal kinetics of LAS in **a** fresh GAC, **b** inactivated biofilm-GAC, **c** bio-enhanced GAC, and **d** the modeling results in the bio-enhanced GAC. The pseudo-first order and the pseudo-second-order models were used for the LAS adsorption kinetics fitting in the fresh GAC and inactivated biofilm-GAC; a two-step removal model including biofilm adsorption and biodegradation was used for the simulation of LAS removal in the bio-enhanced GAC.

both positions enabled the stable and efficient removal of ammonia (Fig. 2c). Moreover, despite the resemblances of the microbial community at the reactor bottom and stratification, including *Thermomicrobia*, *Sphingobacteria*, *Cytophagia*, and *Phycisphaerae*, the relative abundances of the above-mentioned genes at the bottom were much lower than that at the stratification.

Figure 4c shows the relative abundance heatmap of the predominant microbial communities at the order level (>1% in any sample). Biofilm samples in Phase I were clustered together, which should be related to the same inoculation of activated sludge. In Phase II, biofilm bacterial communities at the top of the reactor changed significantly compared with that in Phase I. Bacteria in Phase III-Up and Phase III-Strat were clustered together and largely different from that in Phase I. Moreover, biofilms at the top and stratification of the reactor contained more colorful microbial

species, including aerobic, anoxic, and anaerobic microorganisms, due to the relatively high DO concentrations; but the anaerobic bacteria containing *Desulfovibrionales*, *Rhodospirillales*, and *Oceanospirillales*[25,26] were predominant in the biofilms at the bottom of the reactor in Phases II and III. Results further indicated that DO concentration would significantly affect the succession of microbial community structure in the BhGAC-DBfR; high DO favor the formation of multifarious genes in the aerobic-anoxic-anaerobic biofilm at the top of the reactor[12,27], and low DO favors the formation of anaerobic biofilm[21] and led to the relatively less abundant microbial communities at the bottom of the reactor.

Dynamics of functional genes by metagenomic prediction

Figure 5 shows the predicted functional genes involved in organic nitrogen (ON) and ammonia metabolism, nitrate respiration, and

Table 2. Parameters of the adsorption and biodegradation kinetics during batch-mode LAS removal in various GAC-based systems.

Model	Parameter	Unit	Fresh GAC[a]	Inactivated GAC	Bio-enhanced GAC
Pseudo-first order kinetics	k_1[b]	h^{-1}	0.560	0.551	0.554
	$q_{e,\,mod}$[c]	mg/g	0.169	0.161	0.164
	$q_{e,\,exp}$[d]	mg/g	0.144	0.143	—
	SSE[e]	—	0.034	0.022	—
Pseudo-second-order kinetics	k_2[f]	g/(mg·h)	0.0547	0.0374	—
	$q_{e,\,mod}$	mg/g	0.495	0.584	—
	$q_{e,\,exp}$	mg/g	0.144	0.143	—
	SSE	—	0.086	0.067	—
Biodegradation kinetics	k_{Biod}[g]	h^{-1}	—	—	0.0580

[a]GAC is granular-activated carbon.
[b]k_1 and [f]k_2 are the first and second-order rate constant, respectively.
[c]$q_{e,\,mod}$ and [d]$q_{e,\,exp}$ are the equilibrium adsorption capacity based on modeling and experiment results, respectively.
[e]SSE is the sum of errors' squares.
[g]k_{Biod} is the biodegradation rate constant.

LAS biodegradation in the biofilms at different reactor positions and saturated/unsaturated ratios during graywater treatment. For the metabolism of LAS, all the predicted functional enzymes in the biofilm showed the highest relative abundance at the top of the reactor, but the opposite trend for biofilm at the reactor bottom, indicating that high DO favor the proliferation and accumulation of LAS-biodegrading bacteria that enabled the efficient mineralization of LAS in the biofilm[6,21]. Enzymes, associated with nitrate respiration, including nitrate reductase (NAR), nitrite reductase (NIR), nitric oxide reductase (NOR), nitrous oxide reductase (NOS), and glutamine synthetase[19,28], exhibited the relatively higher abundances. A saturated/unsaturated ratio at 1:0.5 in Phase III showed further led to the highest enzymes abundances for nitrate respiration, which may be related to the lowest DO concentrations in the biofilms at all the target reactor positions (Table 1) that favored the formation of denitrification related bacteria[12,29]. The potential enzymes functional for ON (minor extracellular protease, D-amino-acid oxidase, glutamate dehydrogenase (NAD(p)+), L-serine dehydratase, deoxyribonuclease I, and urease)[30,31] and ammonia metabolism (glutamate dehydrogenases, ammonia monooxygenase (AMO), nitrite oxidoreductase (NXR) and hydroxylamine oxidase)[28,32] mirrored the dynamics of those for LAS metabolisms.

DISCUSSION

Figure 6 shows the functional zones, reactions related to organics and nitrogen removal, and the mass flow of carbon and nitrogen at different positions of the BhGAC-DBfR during graywater treatment. In the unsaturated zone, the organics containing LAS can eventually be oxidized to carbon dioxide (CO_2) by typical aerobic heterotrophs, including Pseudomonadales, Rhodocyclales, Actinomycetales, Sphingobacteriales, c_Betaproteobacteria, Aeromonadales, and Rhizobiales[6,33,34]; ON can be hydrolyzed to NH_4^+-N by the related enzymes functional for ON metabolism (Fig. 5), and NH_4^+-N was further oxidized to NO_2^--N and NO_3^--N by AMO and NXR, respectively in the aerobic layer of the biofilm[28,32]. In the anoxic and anaerobic biofilm inner layers, NO_3^--N can be gradually transformed to N_2 by both aerobic and anaerobic denitrification processes with the functional enzymes of NAR, NIR, NOR, and NOS[32]; in particular, the typical aerobic denitrifying bacteria in this study (Supplementary Fig. 1) mainly include Pseudomonas, Aeromonas, Zoogloea, Comamonas, Acinetobacter, Halomonas, Paracoccus, and Agrobacterium[35,36]. Both of the denitrification processes are also accompanied by the transformation of organic compounds[37]. The oxygen flushing zone can achieve the 81.1% and 85.3% removal of COD and TN in Phase I, respectively, and LAS only contributes 1.2% of the organics in the stratification effluent.

In the Transition zone, the residual ON, nitrate, and nitrite can be removed through the aerobic and anaerobic denitrification process in the anoxic and anaerobic layers of the biofilm on GAC surface (Figs. 4c and 5), and organics can be also further removed in both processes in this zone. In the anaerobic zone at the bottom of the reactor, residual nitrogen and organics can be further removed in the anaerobic denitrification process[12]. The organics and nitrogen can be further reduced to 6.6% and 4.0%, respectively, indicating the 12.3% and 10.4% removal of COD and TN in the sublayer of the reactor. In the effluent, LAS only accounted for 0.97% of organics, and ON contributed 80.3% of the effluent TN, indicating that the refractory nitrogen-containing organics, including humic substances, were the main source of effluent nitrogen[12,38]. The saturated zone can be considered as a polishing step for the continuous removal of organics and nitrogen after the majority of treatment took place in the unsaturated zone[8]. Moreover, because of the manifold functional groups in both GAC and biofilm (Fig. 1g), organics and nitrogen can be quickly absorbed and accumulated in the bio-enhanced GAC located at the target functional zones, both of which can be further removed by the related functional microorganisms and enzymes (Figs. 4c and 5). Key is that adsorption and biodegradation play important and distinct roles in the quick uptake and continuous removal of both organics and N in the BhGAC-DBfR.

During the 5-month operation of BhGAC-DBfR, no blockage occurred for synthetic graywater treatment, but the actual graywater may contain hair, dander, etc., which may cause reactor clogging and affect biofilm stability and pollutants removal performance[39]. Thus, a strainer needs to be installed before the biochemical treatment process in practice. Moreover, graywater contains large amounts of LAS[1,12], which causes the replication of antibiotics resistance genes (ARGs) in the antibiotics resistance bacteria[40] and may further affect the effluent quality of BhGAC-DBfR during graywater treatment; more attention should be focused on the ARGs proliferation, transformation and efficient removal in the BhGAC-DBfR.

In conclusion, we developed an easy-to-maintain and energy-efficient BhGAC-DBfR for source-diverted graywater treatment. Increasing of saturated/ unsaturated ratio led to the continuous growth of biomass on GAC surface. Especially, the highest biofilm components concentration and multifarious function groups were achieved at the top of the reactor. The saturated/unsaturated ratio at 1:1.1 achieved the maximum removal of COD (98.3%), LAS
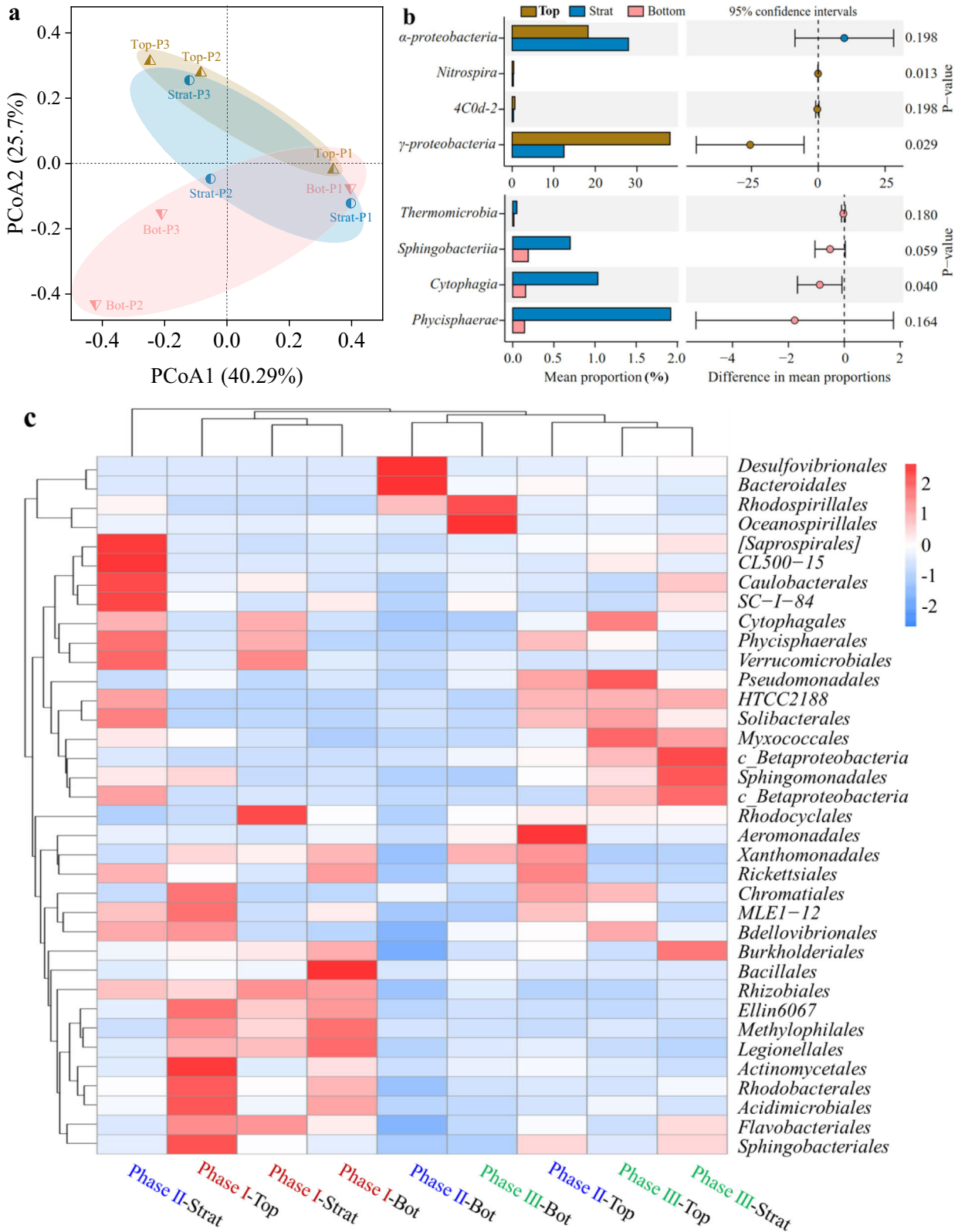
Fig. 4 **Microbial communities.** a PCoA of the Bray-Curtis distance of bacterial communities, **b** the statistically significant differences among the bacterial, and **c** the heatmap of the relative abundances of bacteria genera (>1% in any sample) at genus level at different reactor positions and operation Phases. Start and Bot are stratification and bottom, respectively. One-way ANOVA was applied to evaluate the significance of the differences between samples.
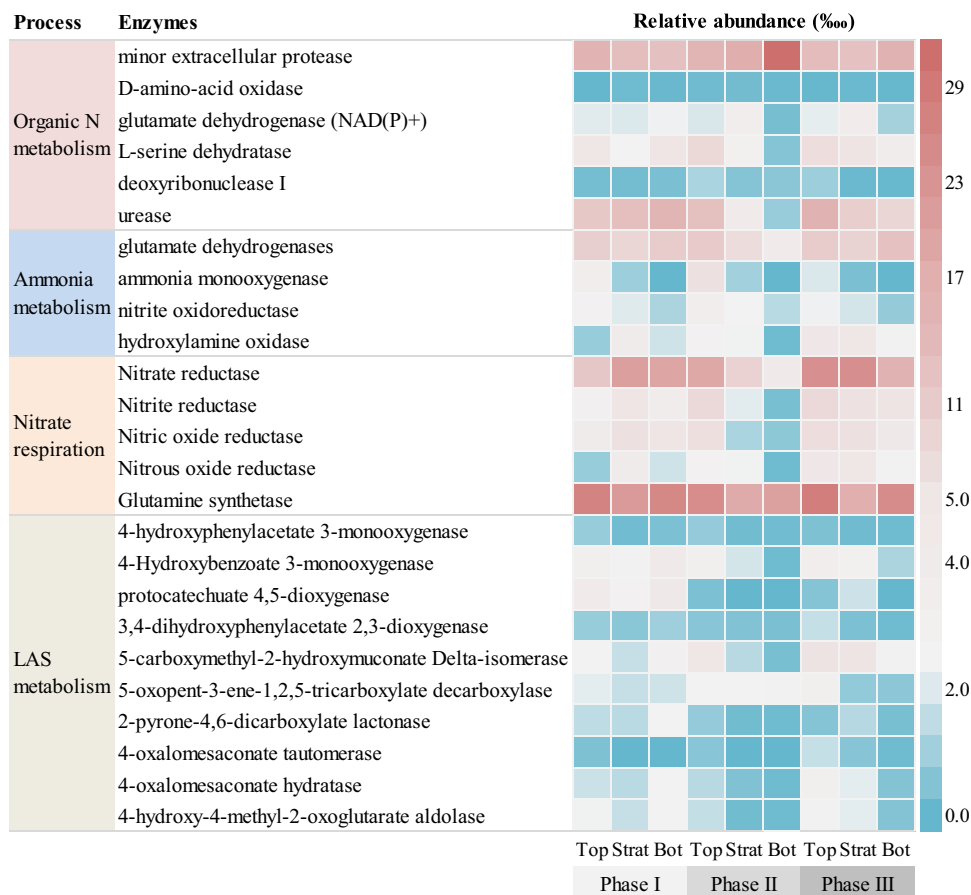
Fig. 5 Dynamics of functional enzymes. Relative abundance of predicted functional enzymes involved in several key metabolisms by PICRUSt analysis in the biofilms of the bio-enhanced granular-activated carbon dynamic biofilm reactor (BhGAC-DBfR) at various saturated/unsaturated ratios during graywater treatment.

(99.4%), ammonia nitrogen (99.8%), and TN (83.5%), most of which were removed in the unsaturated zone. Key is that adsorption and biodegradation play important and distinct roles in the quick uptake and continuous removal of both organics and N in BhGAC-DBfR. Microbial community analysis further elucidated that the related genus and enzymes functional for LAS mineralization, organic N and ammonium metabolisms, and nitrate respiration enabled the efficient and simultaneous removal of organics and N in the system. Consequently, the developed BhGAC-DBfR can offer an easy-to-maintain method to achieve efficient and low-energy-input graywater and other types of wastewater treatment.

METHODS

GW preparation and granular-activated carbon
The synthetic graywater (25× concentration) used in this work was prepared according to the National Sanitation Foundation (NSF)/American National Standards Institute (ANSI) Standard 350[41], which simulates the mixture of bathing and laundry wastewater. GW needs to be diluted for 25 times before using it as reactor feed water. The pH of the feed water was maintained at 7.05 ± 0.05 using 1.0 M NaOH or HCl, and then stored in the fridge at 4 °C before use. Detailed information about the formulation and characteristics of synthetic graywater was shown in Supplementary Tables 1 and 2, respectively.

A commercial acid-washed coconut husk GAC (TingYou, Shanghai, China), with a particle size of 2.0–3.2 mm, was selected as the filter media in the BhGAC-DBfR. The sieved fresh GAC was washed using deionized water to clean off the floating dust before using. The

washed GAC was soaked in diluted activated sludge (AS) for 3 h with the dilution ratio of 10 mL AS (4.56 g TSS/L): 2 L tap water, which enabled the attachment of microorganisms on the GAC surface and accelerated the formation of biofilm for graywater treatment.

Continuous operation of the BhGAC-DBfR
The experiments were conducted in a laboratory-scale cylindrical reactor with an internal diameter and effective height of 6.0 and 67 cm, respectively. A schematic of the BhGAC-DBfR is shown in Fig. 7a. The effective empty volume of the reactor was 1.90 L, which can hold 0.92 L of water when filled with GAC. Graywater was delivered to the top of the reactor by a peristaltic pump (BT100-2J, LongerPump®, China) and distributed evenly through a grid water distributor. The gravity flow of feed GW led to the formation of unsaturated and saturated regions in the BhGAC-DBfR. The depth of the saturated region was controlled by the height of the outlet from the reactor bottom according to the law of connected vessels[8]. For the continuous long-term operation of BhGAC-DBfR, the saturated/unsaturated ratio was controlled at 1:2.3, 1:1.1, and 1:0.5[8], respectively. The hydraulic retention time (HRT) for each phase was maintained at 6.7 h by adjusting the influent pump speed.

Figure 7b shows the functional zones and biofilm layers in the BhGAC-DBfR. The unsaturated zone achieved natural-supplying O_2 of graywater and led to the relatively high dissolved oxygen (DO) concentration in the unsaturated-saturated interface (Table 1). According to DO concentration, the reactor can be divided into three functional zones: oxygen flushing zone (DO > 0.5 mg/L, and the boundary was lower than the unsaturated-saturated interface), transition zone (DO = 0.2–0.5 mg/L), and anaerobic zone
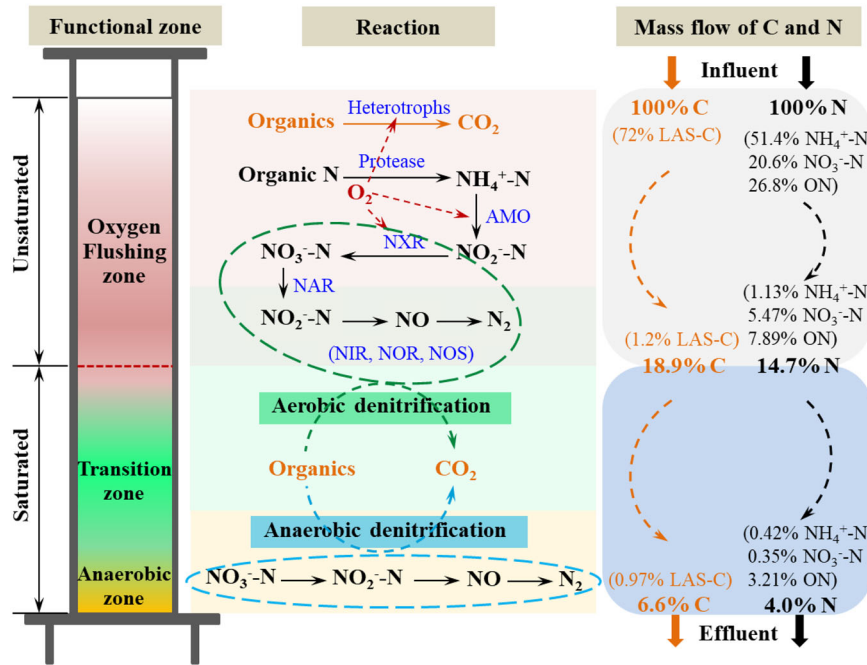
Fig. 6 Carbon and nitrogen mass flows and removal mechanisms. Functional zones, reactions responsible for organics and nitrogen removal, and the mass flow of carbon and nitrogen at different positions of the bio-enhanced granular-activated carbon dynamic biofilm reactor (BhGAC-DBfR) during graywater trearment. The data present in the mass flow panel was obtained from Phase I.

(DO < 0.2 mg/L, mainly exist at the bottom of the reactor). In the unsaturated zone, utilization of O_2 by microorganisms led to the gradually dropped DO concentration from the liquid-biofilm interface to biofilm-GAC interface[6,19], which favored the formation of aerobic-anoxic-anaerobic biofilm[12]. Relatively low DO concentrations in the transition and anaerobic zones favored the formation of anoxic-anaerobic and anaerobic biofilms, respectively[27]. Moreover, increasing in the saturation/unsaturated ratio led to the rise of both hydraulic and organic loading rates, as well as the decrease of DO concentrations in both stratification and effluent (Table 1). The formation of multifunctional biofilm on GAC surface enabled simultaneous and efficient removal of organics and nitrogen in the BhGAC-DBfR[6,12,27].

Batch experiments to differentiate LAS adsorption and biodegradation

In this study, three types of GAC were used to explore the relationships between LAS degradation and adsorption by biofilm and activated carbon: fresh GAC, bio-enhanced GAC, and inactivated biofilm-GAC. The bio-enhanced GAC was obtained from the top of the unsaturated zone in the continuously operated BhGAC-DBfR. The media were collected at the steady state of Phase III (day 140) with a saturated/unsaturated ratio of 1:0.5. Part of the bio-enhanced GAC was completely inactivated using mercuric chloride (30 mg/g dry biomass)[42], which was recorded as the inactivated biofilm-GAC.

In order to differentiate GAC adsorption, biofilm adsorption, and biodegradation of LAS, three identical Erlenmeyer flasks with a volume of 500 mL were used for the batch experiments. Detailed information about the batch-experiment design was shown in Supplementary Fig. 2. Bio-enhanced GAC, inactivated biofilm-GAC, and fresh GAC (with the same wet weight of 135.7 g) combined with 200 mL of triple diluted GW were added into flasks A1, A2, and A3, respectively. The moisture content of the target three types of GAC was almost the same at 60.5%. The experiments were carried out in the Constant Temperature Vibrator (SHZ-82, LICHEN、Shanghai) with the speed of 200 rpm for 24 h at room temperature (21 ± 1 °C). All the flasks were covered with tin foil to

minimize water evaporation[14]. We collected liquid samples at 5, 10, 20, 30 min and 1, 2, 4, 8, 12, 24 h, respectively, which were used for the determination of residual LAS concentrations.

In order to quantify the adsorption of LAS by GAC and inactivated biofilm, the pseudo-first-order equation and the pseudo-second-order equation were used to simulate the experiment results. The pseudo-first and -second-order equations are generally expressed as Eqs. (1) and (2), respectively[43]:

$$\frac{dq_t}{dt} = k_1(q_e - q_t) \tag{1}$$

$$\frac{dq_t}{dt} = k_2(q_e - q_t)^2 \tag{2}$$

where q_e and q_t are equilibrium adsorption capacity and the adsorption capacity (mg/g) at time t (min), separately (mg/g), and k_1 and k_2 are the first (min^{-1}) and second-order rate constant (g/(mg·min)). For LAS biodegradation in the active biofilm, LAS removal rate is related to the biodegradation rate constant (k_{Biod}, min^{-1}) constant and LAS concentration in the biofilm (C_t, mg/L)[17]:

$$\frac{dC_t}{dt} = k_{Biod}C_t \tag{3}$$

The planning solving tool in the Microsoft Excel was used to estimate the parameters (k_1, k_2, k_{Biod}, and q_e) by minimizing the sum of errors' squares (SES) between experimental data (q_{exp}, mg/g) and model predicted values (q_{mod}, mg/g) with the objective function:

$$SES = \sum_{i=1}^{n} \left(q_{exp,i} - q_{mod,i} \right)^2 \tag{4}$$

where $q_{exp,\,i}$ and $q_{mod,\,i}$ are vectors of n experiment data and model predicted values at time t_i (i from 1 to n).

Sample collection and chemical analyses

Liquid samples were collected periodically from the influent, stratification, and effluent in the continuously operated BhGAC-
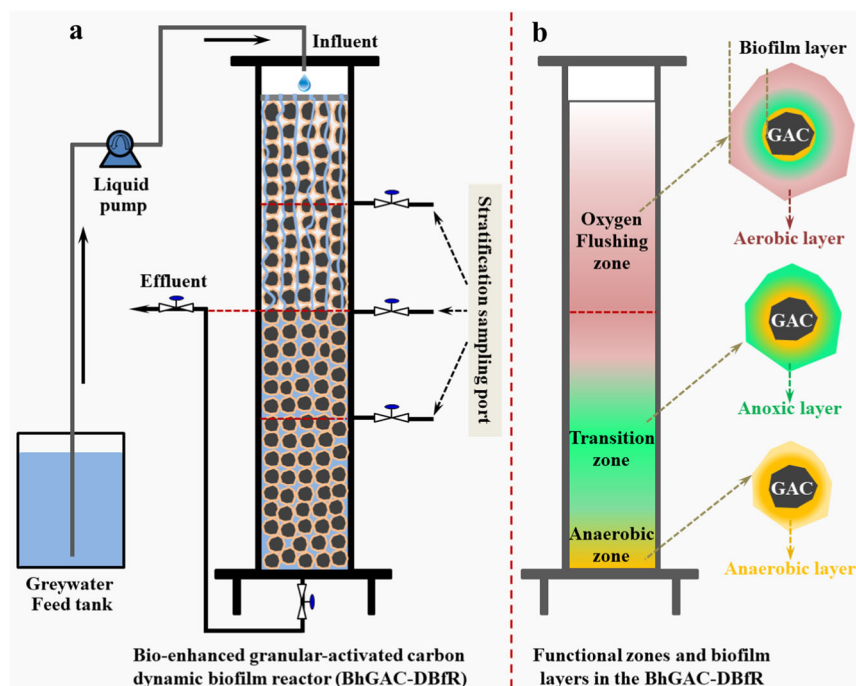
Fig. 7 Experimental setup. Schematic of **a** the bio-enhanced granular-activated carbon dynamic biofilm reactor (BhGAC-DBfR) and **b** the functional zones and biofilm layers in the BhGAC-DBfR at the noted position of stratification (saturated/unsaturated ratio = 1:1.1) during graywater treatment.

DBfR. Samples were stored in 15 mL polypropylene centrifuge tubes (BD Falcon, VWR, USA) at 4 °C (Refrigerator, BCD-528WDPF, Haier, Hefei, China), and used directly for determining of COD, LAS, TN, NH_4^+-N, NO_2^--N, and NO_3^--N concentrations. For the batch experiments, liquid samples were collected at the noted time and directly for the determination of residual LAS concentration.

Biofilm samples were collected at the end of each phase (steady state) from different positions (top, stratification, and bottom, and denoted by $Biof_{Top}$, $Biof_{Strat}$, and $Biof_{Bot}$, respectively) of the BhGAC-DBfR. Part of the biofilm samples was directly used for DNA extraction and high throughput sequencing analysis; part of the biofilm samples was used for biomass components (protein, carbohydrate, and DNA) concentrations determination; part of the biofilm samples were used for surface morphology and the element distribution analyses using a scanning electron microscope (SEM) combined with energy dispersive X-ray (EDX) spectrometry; other parts of biofilm samples were used for Fourier Transform Infra-Red (FTIR) and the two dimension (2D)-FTIR analyses. COD, TN, and NH_4^+-N concentrations were measured according to Standard Methods[44]. Concentrations of NO_2^--N and NO_3^--N were measured using a benchtop spectrophotometer (DR 3900, HACH, USA) with the following HACH kits and reagents: NO_3^--N kits, 2106169-CN (0.3-30.0 mg/L NO_3^--N, HACH, USA), and NitriVer 2 Nitrite Reagent Powder Pillows, 2107169-CN (0.002-0.300 mg/L NO_2^--N, HACH, USA), respectively. LAS concentrations were measured using a methylene blue spectrophotometry[12,18,45]. Influent and effluent pH values were determined using a pH meter (B40PCID, VWR, SympHony). DO concentration was measured using a DO meter (AR8010, SMART SENSOR, Dongguan, China).

Scanning electron microscope (SEM) images and energy dispersive X-ray (EDX) analysis were performed using Philips XL 30 ESEM and EDX spectrometer. The GAC and biofilm were freeze-dried initially, and then the functional groups were analyzed by Fourier transform infrared (FTIR) spectrometer Nicolet 5700. The spectrum was recorded in the wave number range of 600–2000 cm^{-1} at a resolution of 5 cm^{-1} with 16 scans. Two-dimensional correlation spectroscopy (2D-COS) was used to characterize the enhancement of FTIR spectral

resolution and expound on the changes in the chemical structure of biofilm. The reconstructed data matrix was processed by "2D Shige" software (Kansai University, Japan). The concentrations of protein, carbohydrate, and deoxyribonucleic acid (DNA) in the biofilm were determined by the following methods[46]: Coomassie brilliant blue G-250 dye-binding method, using bovine serum albumin as the criteria for protein; phenol sulfuric acid method, glucose as the criteria for carbohydrate; and diphenylamine colorimetry using calf thymus deoxyribonucleic acid as the criteria for DNA.

DNA extraction and microbial community analyses

All the collected biofilm samples at the noted reactor position and operation phase were used for genomic DNA extraction with the DNeasy PowerSoil Kit (Qiagen Inc., Toronto, Canada) according to the manufacturer's protocol. The extracted DNA samples were sent to Shanghai Personalbio technology Co., Ltd (Shanghai, China) for barcoding and sequencing on an Illumina NextSeq 500 platform. QIIME2 version 2018.8[47] was used to process the raw data according to Callahan et al.[48]. In line with the GreenGenes reference database (version 13_5), the taxonomy was assigned with 99% similarity[49]. Principal Coordinates Analysis (PCoA) based on Bray-Curtis distance matrixs was performed using the "vegan" package in R Studio[50]. The related enzymes functional for carbon and nitrogen metabolism in the BhGAC-DBfR were predicted using PICRUSt 2.0 based on the mapping of sequenced 16 S rRNA gene data to the KEGG database[51].

Statistical analysis

The concentrations of COD, LAS, NH_4^+-N, NO_3^--N, NO_2^--N, TN, protein, carbohydrate, and DNA, as well as DO and pH values, were measured in triplicate for each sample. Results are expressed as the mean with the standard deviation (mean ± SD). OriginPro 2022b Beta software (OriginLab Corp, Northampton, USA) was used to conduct statistical analyses. One-way ANOVA was applied to evaluate the significance of the differences between samples. The relationship between two parameters was considered statistically significant with a 95% confidence interval ($P < 0.05$).

REFERENCES
1. Shaikh, I. N., Ahammed, M. M. & Krishnan, M. P. S. Graywater treatment and reuse. in *Sustainable Water and Wastewater Processing*, 19–54 (Elsevier, 2019).
2. Kim, S. & Park, C. Potential of ceramic ultrafiltration membranes for the treatment of anionic surfactants in laundry wastewater for greywater reuse. *J. Water. Process. Eng.* **44**, 102373 (2021).
3. Ghaitidak, D. M. & Yadav, K. D. Characteristics and treatment of greywater—a review. *Environ. Sci. Pollut. Res.* **20**, 2795–2809 (2013).
4. Shaikh, I. N. & Ahammed, M. M. Quantity and quality characteristics of greywater: a review. *J. Environ. Manag.* **261**, 110266 (2020).
5. Shreya, Verma, A. K., Dash, A. K., Bhunia, P. & Dash, R. R. Removal of surfactants in greywater using low-cost natural adsorbents: a review. *Surf. Interfaces* **27**, 101532 (2021).
6. Zhou, Y. et al. Treatment of grey water (GW) with high linear alkylbenzene sulfonates (LAS) content and carbon/nitrogen (C/N) ratio in an oxygen-based membrane biofilm reactor (O2-MBfR). *Chemosphere* **258**, 127363 (2020).
7. Ren, X., Zhang, Y. & Chen, H. Graywater treatment technologies and reuse of reclaimed water for toilet flushing. *Environ. Sci. Pollut. Res.* **27**, 34653–34663 (2020).
8. Sharaf, A., Guo, B., Shoults, D. C., Ashbolt, N. J. & Liu, Y. Viability of a single-stage unsaturated-saturated granular activated carbon biofilter for greywater treatment. *Sustainability* **12**, 8847 (2020).
9. Hug, T. Characterization and controlling of foam and scum in activated sludge systems. ETH Zurich (2006).
10. Rosso, D., Larson, L. E. & Stenstrom, M. K. Aeration of large-scale municipal wastewater treatment plants: state of the art. *Water Sci. Technol.* **57**, 973–978 (2008).
11. Rittmann, B. E. The membrane biofilm reactor is a versatile platform for water and wastewater treatment. *Environ. Eng. Res.* **12**, 157–175 (2007).
12. Zhou, Y. et al. Greywater treatment using an oxygen-based membrane biofilm reactor: Formation of dynamic multifunctional biofilm for organics and nitrogen removal. *Chem. Eng. J.* **386**, 123989 (2020).
13. Lu, Z. et al. Implication on selection and replacement of granular activated carbon used in biologically activated carbon filters through meta-omics analysis. *Water Res.* **198**, 117152 (2021).
14. Sharaf, A. & Liu, Y. Mechanisms and kinetics of greywater treatment using biologically active granular activated carbon. *Chemosphere* **263**, 128113 (2021).
15. Huggins, T. M., Haeger, A., Biffinger, J. C. & Ren, Z. J. Granular biochar compared with activated carbon for wastewater treatment and resource recovery. *Water Res.* **94**, 225–232 (2016).
16. Zhang, Y. et al. Granular activated carbon stimulated microbial physiological changes for enhanced anaerobic digestion of municipal sewage. *Chem. Eng. J.* **400**, 125838 (2020).
17. Cui, X., Ren, Q., Zhang, J. & Zhou, Y. Removal kinetics of linear alkylbenzene sulfonate in a batch-operated oxygen based membrane biofilm reactor treating greywater: quantitative differentiation of adsorption and biodegradation. *Sci. Total Environ.* **806**, 150523 (2022).
18. Zhou, Y. et al. Promoting waste activated sludge reduction by linear alkylbenzene sulfonates: Surfactant dose control extracellular polymeric substances solubilization and microbial community succession. *J. Hazard. Mater.* **374**, 74–82 (2019).
19. Zhou, Y. et al. The influent COD/N ratio controlled the linear alkylbenzene sulfonate biodegradation and extracellular polymeric substances accumulation in an oxygen-based membrane biofilm reactor. *J. Hazard. Mater.* **422**, 126862 (2022).
20. Noda, I. Advances in two-dimensional correlation spectroscopy. *Vibrational Spectrosc.* **36**, 143–165 (2004).
21. Zhou, Y. et al. Lumen air pressure (LAP) affecting greywater treatment in an oxygen-based membrane biofilm reactor (O2-MBfR). *Chemosphere* **270**, 129541 (2021).
22. Yuan, J., Passeport, E. & Hofmann, R. Understanding adsorption and biodegradation in granular activated carbon for drinking water treatment: a critical review. *Water Res.* **210**, 118026 (2022).
23. Mittal, A. Use of hen feathers as potential adsorbent for the removal of a hazardous dye, Brilliant Blue FCF, from wastewater. *J. Hazard. Mater.* **128**, 233–239 (2006).
24. Vlaeminck, S. E. et al. Nitrogen removal from digested black water by one-stage partial nitritation and anammox. *Environ. Sci. Technol.* **43**, 5035–5041 (2009).
25. Zhou, Y. et al. Anaerobically digested blackwater treatment by simultaneous denitrification and anammox processes: Feeding loading affects reactor performance and microbial community succession. *Chemosphere* **241**, 125101 (2020).
26. Luostarinen, S., Sanders, W., Kujawa-Roeleveld, K. & Zeeman, G. Effect of temperature on anaerobic treatment of black water in UASB-septic tank systems. *Bioresour. Technol.* **98**, 980–986 (2007).
27. Zhou, Y. et al. Three-dimension oxygen gradient induced low energy input for greywater treatment in an oxygen-based membrane biofilm reactor. *Environ. Res.* **191**, 110124 (2020).
28. Liu, Z. et al. Accurate O2 delivery enabled benzene biodegradation through aerobic activation followed by denitrification-coupled mineralization. *Biotechnol. Bioeng.* **115**, 1988–1999 (2018).
29. Zhou, Y., Li, R., Guo, B., Yu, N. & Liu, Y. Cometabolism accelerated simultaneous ammoxidation and organics mineralization in an oxygen-based membrane biofilm reactor treating greywater under low dissolved oxygen conditions. *Sci. Total Environ.* **789**, 147898 (2021).
30. Le Roux, M. R., Khan, S. & Valentine, A. J. Organic acid accumulation may inhibit N2 fixation in phosphorus-stressed lupin nodules. *N. Phytol.* **177**, 956–964 (2008).
31. Tian, X. et al. Ammonium detoxification mechanism of ammonium-tolerant duckweed (Landoltia punctata) revealed by carbon and nitrogen metabolism under ammonium stress. *Environ. Pollut.* **277**, 116834 (2021).
32. Ji, B., Zhang, M., Gu, J., Ma, Y. & Liu, Y. A self-sustaining synergetic microalgal-bacterial granular sludge process towards energy-efficient and environmentally sustainable municipal wastewater treatment. *Water Res.* **179**, 115884 (2020).
33. Okada, D. Y., Delforno, T. P., Etchebehere, C. & Varesche, M. B. A. Evaluation of the microbial community of upflow anaerobic sludge blanket reactors used for the removal and degradation of linear alkylbenzene sulfonate by pyrosequencing. *Int. Biodeterior. Biodegrad.* **96**, 63–70 (2014).
34. Andrade, M. V. F., Sakamoto, I. K., Corbi, J. J., Silva, E. L. & Varesche, M. B. A. Effects of hydraulic retention time, co-substrate and nitrogen source on laundry wastewater anionic surfactant degradation in fluidized bed reactors. *Bioresour. Technol.* **224**, 246–254 (2017).
35. Fu, G., Yu, T., Huangshen, L. & Han, J. The influence of complex fermentation broth on denitrification of saline sewage in constructed wetlands by heterotrophic nitrifying/aerobic denitrifying bacterial communities. *Bioresour. Technol.* **250**, 290–298 (2018).
36. Rajta, A., Bhatia, R., Setia, H. & Pathania, P. Role of heterotrophic aerobic denitrifying bacteria in nitrate removal from wastewater. *J. Appl. Microbiol.* **128**, 1261–1278 (2020).
37. Du, R. et al. Advanced nitrogen removal with simultaneous Anammox and denitrification in sequencing batch reactor. *Bioresour. Technol.* **162**, 316–322 (2014).
38. Zhang, Z., Zhou, Y., Zhang, J., Xia, S. & Hermanowicz, S. W. Effects of short-time aerobic digestion on extracellular polymeric substances and sludge features of waste activated sludge. *Chem. Eng. J.* **299**, 177–183 (2016).
39. Ribeiro dos Santos, P., de Souza Leite, L. & Daniel, L. A. Performance of biological activated carbon (BAC) filtration for the treatment of secondary effluent: a pilot-scale study. *J. Environ. Manag.* **302**, 114026 (2022).
40. Scott, L. C. et al. Assessing visitor use impact on antibiotic resistant bacteria and antibiotic resistance genes in soil and water environments of Rocky Mountain National Park. *Sci. Total Environ.* **785**, 147122 (2021).
41. National Sanitation Foundation (NSF)/American National Standards Institute (ANSI) Standard 350, Onsite residential and commercial water reuse treatment systems. NSF International Standard/American. National Standard. (2011).
42. Hamon, P., Villain, M. & Marrot, B. Determination of sorption properties of micropollutants: What is the most suitable activated sludge inhibition technique to preserve the biomass structure? *Chem. Eng. J.* **242**, 260–268 (2014).
43. Ho, Y. S. & McKay, G. A comparison of chemisorption kinetic models applied to pollutant removal on various sorbents. *Process Saf. Environ. Prot.* **76**, 332–340 (1998).
44. APHA. *Standard Methods for The Examination of Water and Wastewater,* 20th edn. (American Public Health Association, Washington, 2017).
45. Zhou, Y. et al. The influent COD/N ratio controlled the linear alkylbenzene sulfonate biodegradation and extracellular polymeric substances accumulation in an oxygen-based membrane biofilm reactor. *J. Hazard Mater.* **422**, 126862 (2022).
46. Frolund, B., Palmgren, R., Keiding, K. & Nielsen, P. H. Extraction of extracellular polymers from activated sludge using a cation exchange resin. *Water Res.* **30**, 1749–1758 (1996).
47. Caporaso, J. G. et al. QIIME allows analysis of high-throughput community sequencing data. *Nat. Methods* **7**, 335–336 (2010).
48. Callahan, B. J. et al. DADA2: High-resolution sample inference from Illumina amplicon data. *Nat. Methods* **13**, 581–583 (2016).

49. Werner, J. J. et al. Impact of training sets on classification of high-throughput bacterial 16s rRNA gene surveys. *ISME J.* **6**, 94–103 (2012).

50. Oksanen, J. & others, *Community ecology package: ordination methods, diversity analysis and other functions for community and vegetation ecologists. Version: 2.4-2.* https://CRAN.Rproject.org/package=vegan (2017).

51. Douglas, G. M. et al. PICRUSt2 for prediction of metagenome functions. *Nat. Biotechnol.* **38**, 685–688 (2020).

AUTHOR CONTRIBUTIONS

Z.W.: conceptualization, methodology, software, formal analysis, writing—original draft; Y.Y.: conceptualization, methodology, software, formal analysis, writing—original draft; W.X.: conceptualization, methodology, software, formal analysis, writing—original draft; B.W.: methodology, review and editing, software; X.C.: methodology, review and editing, software; Y.Z.: conceptualization, writing—review and editing, supervision, project administration. All authors reviewed the manuscript.

COMPETING INTERESTS

The authors declare no competing interests.

ADDITIONAL INFORMATION

Supplementary information The online version contains supplementary material available at https://doi.org/10.1038/s41545-022-00198-7.

Correspondence and requests for materials should be addressed to Yun Zhou.

Reprints and permission information is available at http://www.nature.com/reprints

Publisher's note Springer Nature remains neutral with regard to jurisdictional claims in published maps and institutional affiliations.